

Polymerization Mechanism of Conjugated Dienes in the Presence of Ziegler–Natta Type Catalysts: Theoretical Study of Butadiene and Isoprene Polymerization with CpTiCl_3 –MAO Initiator

Andrea Peluso,^{*,†} Roberto Improta,[‡] and Adolfo Zambelli[†]

Dipartimento di Chimica, Università di Salerno, Via S. Allende, I-84081, Baronissi, Salerno, Italy, and Cattedra di Chimica Teorica, Università Federico II, Via Mezzocannone 4, I-80134 Napoli, Italy

Received November 19, 1998

The mechanism of butadiene and isoprene polymerization in the presence of CpTiCl_3 –MAO has been investigated by means of ab initio computations. According to experimental evidence, the catalytically active species are assumed to be $[\text{CpTi-P}]^+$ organotitanium cations (P = growing polymer chain). The results show that (i) in the active species, P is coordinated to Ti both with the π allyl group of its ending unit and with the π bond of the penultimate unit; (ii) the $\text{cis } \eta^4$ coordination of an incoming monomer to the active species requires the breakage of the latter interaction and the change of the allyl coordination mode from η^3 to η^1 . That significant rearrangement of P is predicted to be the rate-determining step of the whole propagation reaction and is predicted to be much easier when the ending unit of P is butenyl rather than 2-methylbutenyl. That finding accounts both for the large difference observed in the homopolymerization rates of butadiene and isoprene and for the fact that in copolymerizations the two monomers exhibit almost the same reactivity.

Introduction

The mechanistic aspects of Ziegler–Natta catalysis¹ have been the subject of several theoretical papers in the past decade.² Most of them have considered the polymerization of monoalkenes, mostly ethylene and propene, while relatively little attention has been devoted to polymerization of conjugated dienes,^{3–5} despite its relevance for the production of synthetic rubber,⁶ and it represents, from a mechanistic point of

view, one of the most interesting and challenging subjects in the field of transition metal-promoted reactions, for the variety of structurally different products, characterized by a high chemo- and stereoregularity.⁷

As for monoalkenes,⁸ the polymerization of conjugated dienes is believed to occur in two steps: coordination of the incoming monomer (M) to the active species and subsequent insertion into the metal–allyl bond. However, in the case of conjugated diolefins, the polymerization mechanism is much more complicated, because both the growing polymer chain and M can be coordinated to the metal center in different ways, which can give rise to different insertion pathways, leading to different products.

First, the ending unit of the growing polymer chain, hereafter indicated by R, is an allyl group, and therefore the insertion of M into the metal–allyl bond may occur at either of the two ending allyl carbons, leading to the products of 1,4 or 1,2 polymerization, cf. Scheme 1.

In addition, the allyl group can be coordinated in the syn or anti forms, as shown in Scheme 2, yielding, in the case of 1,4 polymerization, trans or cis polymers,

(1) For a recent review see: Brintzinger, H. H.; Fischer, D.; Müllhaupt, R.; Rieger, B.; Waymouth, R. M. *Angew. Chem., Int. Ed. Engl.* **1995**, *34*, 1143–1170.

(2) (a) Weiss, H.; Ehrig, M.; Ahlrichs, R. *J. Am. Chem. Soc.* **1994**, *116*, 4919. (b) Woo, T. K.; Fan, L.; Ziegler, T. *Organometallics* **1994**, *13*, 2252. (c) Lohrenz, J. C. W.; Woo, T. K.; Ziegler, T. *J. Am. Chem. Soc.* **1995**, *117*, 12793. (d) Margl, P.; Lohrenz, J. C. W.; Ziegler, T.; Blöchl, P. E. *J. Am. Chem. Soc.* **1996**, *118*, 4434. (e) Kawamura-Kuribayashi, H.; Koga, N.; Morokuma, K. *J. Am. Chem. Soc.* **1992**, *114*, 2359, 8687. (f) Castonguay, L. A.; Rappé, A. K. *J. Am. Chem. Soc.* **1992**, *114*, 5832. (g) Yoshida, T.; Koga, N.; Morokuma. *Organometallics* **1994**, *13*, 42. (h) Bierwagen, E. P.; Bercaw, J. C.; Goddard, W. A., III. *J. Am. Chem. Soc.* **1994**, *116*, 1481. (i) Meier, R. J.; van Doremale, G. H. J.; Iarlori, S.; Buda, F. *J. Am. Chem. Soc.* **1994**, *116*, 7274. (j) Sieghbhan, P. E. M. *Chem. Phys. Lett.* **1993**, *205*, 290. (k) Støvneng, J.; Rytter, E. J. *J. Organomet. Chem.* **1996**, *519*, 277. (l) Woo, T. K.; Margl, P.; Lohrenz, J. C. W.; Blöchl, P. E.; Ziegler, T. *J. Am. Chem. Soc.* **1996**, *118*, 13021. (m) Musaev, D. G.; Froese, R. D. J.; Svensson, M.; Morokuma, M. *J. Am. Chem. Soc.* **1997**, *119*, 367. (n) Woo, T. K.; Margl, P.; Ziegler, T.; Blöchl, P. E. *J. Am. Chem. Soc.*, in press. (o) Deng, L.; Woo, T. K.; Cavallo, L.; Margl, P. M.; Ziegler, T. *J. Am. Chem. Soc.* **1997**, *119*, 6177. (p) Cavallo, L.; Guerra, G.; Corradini, P. *J. Am. Chem. Soc.* **1998**, *120*, 2428. (q) Bernardi, F.; Bottoni, A.; Miscione, G. P. *Organometallics* **1998**, *17*, 16–24.

(3) (a) Peluso, A.; Improta, R.; Zambelli, A. *Macromolecules* **1997**, *30*, 2219. (b) Improta, R.; Garzillo, C.; Peluso, A. *THEOCHEM* **1998**, *426*, 249–255.

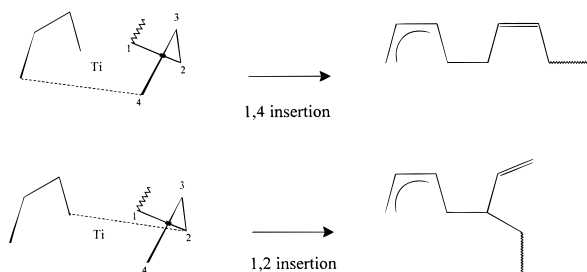
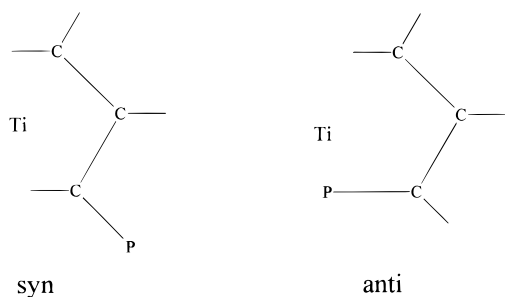
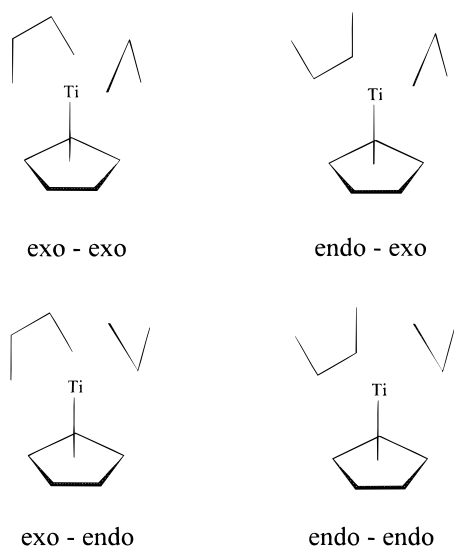
(4) (a) Tobisch, S.; Bogel, H.; Taube, R. *Organometallics* **1996**, *15*, 3563. (b) Boegel, H.; Tobisch, S. *Int. J. Quantum Chem.: Quantum Chem. Symp.* **1996**, *30*, 197–205.

(5) (a) Guerra, G.; Cavallo, L.; Corradini, P.; Fusco, R. *Macromolecules* **1997**, *30*, 678. (b) Guerra G., Cavallo L., private communication.

(6) *Ullmann's Encyclopedia of Industrial Chemistry*; Elvers, B., Hawkins, S., Russell, W., Shulz, G., Eds.; VCH: Weinheim, 1993; Vol. 23.

(7) (a) Porri, L.; Giarrusso, A.; Ricci, G. *Prog. Polym. Sci.* **1991**, *16*, 405. (b) Porri, L.; Giarrusso, A.; Conjugated diene polymerization. In *Comprehensive Polymer Science*; Eastmond, G. C., Ledwith, A., Russo, S., Sigwalt, P., Eds.; Pergamon Press: Oxford, 1989; Vol. 4, Part II, pp 53–108. (c) Theyssie, Ph.; Julemont, M.; Thomassin, J. M.; Walkiers, E.; Warin, R. In *Coordination Polymerization*; Chien, J. C. W., Ed.; Academic Press: New York, 1975; p 327. (d) Boor, J., Jr. In *Ziegler–Natta Catalysts and Polymerizations*; Academic Press: New York, 1979.

(8) Cossee, P. *J. Catal.* **1964**, *3*, 80. Arlman, E. J.; Cossee, P. *J. Catal.* **1964**, *3*, 99.

Scheme 1**Scheme 2****Scheme 3**

respectively.⁷ It has been suggested that the insertion of M coordinated to the metal as a cis η^4 ligand yields the anti form, whereas the trans coordination gives the syn form.⁷ The latter is believed to be thermodynamically preferred for allyls not substituted at C₂, but the anti form can be the predominant one for kinetic reasons,⁹ since the cis η^4 coordination is expected to be more stable than the trans one.

Finally, the stereoselectivity of the reaction has been traced back to the mutual orientation of M and R. It has been suggested that in the 1,2 polymerization of 1,3-(Z)-pentadiene promoted by CpTiCl₃-MAO (Cp = cyclopentadienyl, MAO = methylaluminoxane) an exo-exo (prone-prone) or endo-endo (supine-supine) arrangement of M and R with respect to the Cp ring, cf. Scheme 3, produces syndiotactic polymers, whereas the exo-endo or the endo-exo one gives isotactic polymers.⁷

In such a wide scenario, there are many points worthy of investigation. A general open question concerns the chemical and physical factors that determine the observed chemo- and stereoselectivity of the propagation reaction, but there are also many other puzzling results whose explanation could be of interest, because they could provide guidelines for a deeper understanding of the polymerization mechanism. To cite just a few, there is the case of the highly selective polymerization of pentadiene with CpTiCl₃ activated by MAO, which gives the cis 1,4 polymer at room temperature, with a relatively low rate, and the 1,2 syndiotactic polymer with higher rate at -20 °C,¹⁰ and the case of the very different homopolymerization rates of butadiene and isoprene, a peculiarity of many homogeneous organometallic catalysts,¹¹⁻¹⁶ particularly of CpTiCl₃-MAO, in the presence of which the homopolymerization rates differ by 2-3 orders of magnitude, despite the fact that in copolymerizations the two monomers exhibit almost the same reactivity.¹⁷

In this paper we report the results of a comparative study of the homopolymerization and copolymerization of butadiene and isoprene in the presence of CpTiCl₃-MAO, done with the intention of understanding the factors that make the homopolymerization of butadiene much faster than that of isoprene. Although we will refer to a specific problem and to a particular catalytic system, the results reported here should provide useful hints to clarify general aspects of the mechanisms of conjugated diene polymerization with transition metal-based catalysts.

Preliminary Considerations

CpTiX₃-MAO is one of the most studied Ziegler-Natta catalysts, promoting polymerization of ethylene and α olefins,¹⁸ conjugated diolefins,^{7,17} styrene, and substituted styrenes.¹⁹ In the presence of that catalytic system, polymerization of conjugated diolefins and of styrenes is stereospecific, producing, for example, 1,4 cis polymers of 1,3-butadiene and isoprene¹⁷ and 1,2-syndiotactic polymers of styrene and substituted styrenes¹⁹ and of 4-methyl-1,3-pentadiene.²⁰ There is substantial evidence that the active species promoting polymerization of both conjugated diolefins and styrenes are [CpTi-P]⁺ cations (P = growing polymer chain),

(10) Ricci, G.; Italia, S.; Giarrusso, A.; Porri, L. *J. Organomet. Chem.* **1993**, 451, 67-72. (b) Ricci, G.; Italia, S.; Porri, L. *Macromolecules* **1994**, 27, 868-869.

(11) Pasquon, I.; Porri, L.; Zambelli, A.; Ciampelli, F. *Chim. Ind.* **1963**, 43, 509.

(12) 16 Powell, J. *J. Chem. Soc. A* **1971**, 2233.

(13) Hughes, R. P.; Powell, J. *J. Am. Chem. Soc.* **1972**, 94, 7723.

(14) (a) Henderson, J. F. *J. Polym. Sci., Part C* **1963**, 4, 233. (b) Marconi, W.; Araldi, M.; Beranger, A.; De Maldè, M. *Chim. Ind.* **1963**, 45, 522.

(15) (a) Natta, G.; Porri, L.; Mazzeo, A. *Chim. Ind.* **1959**, 41, 398; (b) **1959**, 41, 116.

(16) Druz, N. N.; Zak, A. V.; Lobach, M. I.; Shpakov, P. P.; Kormer, V. A. *Eur. Polym. J.* **1977**, 13, 875.

(17) (a) Oliva, L.; Longo, P.; Grassi, A.; Ammendola, P.; Pellicchia, C. *Makromol. Chem. Rapid Commun.* **1990**, 11, 519. (b) Zambelli, A.; Proto, A.; Longo, P.; Oliva, P. *Macromol. Chem. Phys.* **1994**, 195, 2623.

(18) Kaminski, W.; Min, M.; Sinn, H.; Woldt, R. *Makromol. Chem. Rapid Commun.* **1983**, 4, 417.

(19) (a) Ishihara, N.; Kuramoto, M.; Uoi, M. *Macromolecules* **1988**, 21, 3356. (b) Zambelli, A.; Oliva, L.; Pellicchia, C. *Macromolecules* **1989**, 22, 2129.

(20) (a) Zambelli, A.; Ammendola, P.; Proto, A. *Macromolecules* **1989**, 22, 2186. (b) Porri, L.; Galeazzi, M. C. *Eur. Polym. J.* **1966**, 2, 189.

(9) Taube, R.; Gehrke, J. P.; Schmidt, U. *Makromol. Chem. Macromol. Symp.* **1986**, 3, 389.

ligands other than Cp probably being removed from the coordination sphere of Ti by MAO.^{21–23} Thus, for CpTiX₃ activated by MAO, the effect of the counterion is expected to be less important than for other Ziegler–Natta type catalysts, as for instance for tight ion pairs; however we warn the reader about the limitation of the model systems we will use in computations, which omit the counterion.

The X-ray structures of some complexes of conjugated diolefins, allyls, styrene, and substituted styrenes with Cp–Zr cations, which could represent reasonable structural models for possible intermediates of the reaction mechanism, have also been reported.^{24,25}

As cited above, R and M can be coordinated to Ti in several ways, so that one should start by finding out the preferred nuclear configurations of the active catalytic species [Cp–Ti(R)]⁺ and of the preinsertion intermediate [Cp–Ti(R)(M)]⁺. However, an analysis of the structural data available in the literature and of the polymerization products allows us to discard some of the possible combinations. In the presence of CpTiCl₃–MAO the polymerization of butadiene and isoprene yields 1,4 cis polymers,¹⁷ suggesting that the ending unit of R is in the anti form. Moreover, previous computations at the ab initio UHF level of theory, with Møller Plesset second-order (MP2) corrections, have shown that for R = butenyl and isoprenyl the syn and the anti forms are very close in energy, with a slight preference for the anti form, ca. 1.5 kcal/mol, for R = butenyl.³

As concerns the orientation of R and M with respect to the cyclopentadienyl ligand, there is some experimental and theoretical evidence that would indicate that the endo–endo or the exo–exo forms are the preferred ones. The X-ray structure of CpZr(allyl)(butadiene) complex has shown that the allyl and the diene ligands prefer to be both in the endo or both in the exo orientation with respect to the Cp ring.²⁵ Accordingly, in the presence of CpTiX₃–MAO, the polymerization of 1,3-(*Z*)-pentadiene produces 1,2-syndiotactic polymers, which should require an exo–exo or endo–endo arrangement of R and M.⁷ Thus considering that molecular mechanics would suggest that the reaction is easier for an endo–endo arrangement⁵ and that this result is fully confirmed by computations based on density functional theory (DFT), according to which the exo–exo arrangement is ruled out for the much higher barrier for insertion (ca. 15 kcal/mol higher than the endo–endo one),^{5b} we will start by keeping R in the anti form and both R and M in the endo orientation with respect to the Cp ring.

Finally, it is possible that the highly electron deficient Ti ion is also coordinated to the penultimate unit of R, which has two π electrons to form a dative bond, the so-called back-biting interaction.^{26–29} This interaction is expected to be strong and can significantly influence

all the steps of the polymerization mechanism. Therefore, we have preferred to use a more realistic model for the growing polymer chain, which in the present study has been modeled by two repeating units, rather than adopting a more sophisticated and reliable computational approach on a simplified model.

Computational Details

All computations have been carried out at the ab initio level of theory using the all-electron ROHF approximation and the standard 6-31G basis set for carbons and hydrogens and a triple- ζ valence basis for titanium,³⁰ except for the starting points of geometry optimizations, namely the transition states for M insertion into Ti–allyl bond, which have been estimated using the 3-21G basis set. Several tests carried out with the UHF approximations have given results very similar to those obtained with the ROHF approximation, both for the optimized geometries of stationary states of the potential energy hypersurface (PES) and for energy differences.³¹ Locations of stationary points (minima and maxima) of the potential energy hypersurface (PES) have been carried out by using an analytical gradient/numerical Hessian according to standard algorithms. No constraints have been imposed in the optimization runs. The effects of the electronic correlation on the relative energies have been taken into account by evaluating MP2 energy contributions³² on the stationary geometries predicted at the HF level. The basis set superposition error (BSSE) has been evaluated according to Bernardi's and Boys' procedure,³³ at both the HF and MP2 level of theory, since it may significantly increase when the MP2 approach is used.³⁴ All computations have been carried out with the Gamess package.³⁵

The large size of the systems considered has not made it possible to take more properly into account the effects of electron correlation. The latter may have a significant influence on the predicted relative energies of the stationary states occurring along the reaction path for coordination of M and its insertion into the Ti–R bond, but according to previous studies on polymerization of monoalkenes in the presence of Ziegler–Natta type catalysts, the minimum energy configurations predicted at the Hartree–Fock (HF) level are sufficiently reliable;^{2a} that should be sufficient for our purposes. The only remarkable differences between the SCF geometries and those predicted at the correlated level are the orientations of methyl groups, which form agostic interactions with the metal ion. These weak interactions are underestimated at the HF level, but this drawback should not be too serious in the polymerization of diolefins, since agostic interactions are expected to play a marginal role, as suggested by experiments performed with deuterated monomers.³⁶

The accuracy of the chosen computational method has been accurately tested, with special attention to the predicted

(21) Zambelli, A.; Pellecchia, C.; Oliva, L.; Longo, P.; Grassi, A. *Makromol. Chem.* **1991**, *192*, 223.

(22) Pellecchia, C.; Longo, P.; Proto, A.; Zambelli, A. *Makromol. Chem. Rapid Commun.* **1992**, *13*, 265.

(23) Zambelli, A.; Oliva, L.; Pellecchia, C. *Macromolecules* **1993**, *22*, 2129–2130.

(24) (a) Pellecchia, C.; Immirzi, A.; Pappalardo, D.; Peluso, A. *Organometallics* **1994**, *13*, 3773. (b) Pellecchia, C.; Grassi, A.; Immirzi, A. *J. Am. Chem. Soc.* **1993**, *115*, 1160.

(25) (a) Erker, G.; Berg, K.; Krüger, C.; Müller, G.; Angermund, K.; Benn, R.; Schroth, G. *Angew. Chem., Int. Ed. Engl.* **1984**, *23c*, 455. (b) Erker, G. *J. Organomet. Chem.* **1990**, *400*, 185.

(26) Hughes, R. P.; Jack, T.; Powell, J. J. *Organomet. Chem.* **1973**, *63*, 451–459.

(27) Ciajolo, R.; Jama, M. A.; Tuzi, A.; Vitagliano, A. *J. Organomet. Chem.* **1985**, *295*, 233–238.

(28) Taube, R.; Wache, S. *J. Organomet. Chem.* **1992**, *428*, 431–442.

(29) Allegra, G.; Lo Giudice, F.; Natta, G.; Giannini, U.; Fagherazzi, G.; Pino, P. *Chem. Commun.* **1967**, 1263.

(30) (a) Binkley, J. S.; Pople, J. A.; Hehre, W. J. *J. Am. Chem. Soc.* **1980**, *102*, 939–947. (b) Dobbs, K. D.; Hehre, W. J. *J. Comput. Chem.* **1987**, *8*, 861–879. (c) Wachters, A. J. H. *J. Chem. Phys.* **1970**, *52*, 1033.

(31) Improta, R. Ph.D. Thesis, Università "Federico II", Naples, 1997.

(32) Møller, C.; Plesset, M. S. *Phys. Rev.* **1934**, *46*, 618.

(33) Boys, S. F.; Bernardi, F. *Mol. Phys.* **1970**, *19*, 553.

(34) Axe, F. U.; Coffin, J. M. *J. Phys. Chem.* **1994**, *98*, 2567.

(35) Schmidt, M.; Baldridge, K. K.; Boatz, J. A.; Elbert, S. T.; Gordon, M. S.; Jensen, J. J.; Koseki, S.; Matsunaga, M.; Nguyen, K. A.; Su, S.; Windus, T. L.; Dupuis, M.; Montgomery, J. A. *J. Comput. Chem.* **1993**, *14*, 1347.

(36) Longo, P.; Guerra, G.; Grisi, F.; Pizzuti, S.; Zambelli, A. *Macromol. Chem. Phys.* **1998**, *199*, 149–154.

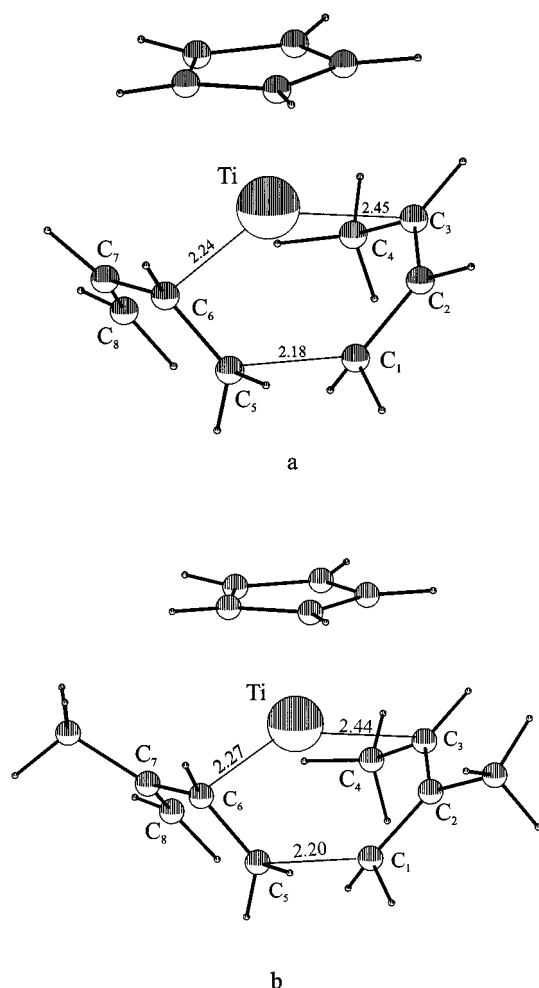


Figure 1. Transition states for insertion of (a) butadiene into the CpTi–butenyl bond and (b) isoprene into the CpTi–isoprenyl bond, obtained at the ROHF/3-21G level. Selected geometrical parameters (Å and deg): (a) Ti–C₁ = 2.48, Ti–C₂ = 2.41, Ti–C₄ = 2.84, Ti–C₅ = 2.63, Ti–C₇ = 2.52, Ti–C₈ = 2.81, C₁–C₂ = 1.45, C₂–C₃ = 1.35, C₆–C₇ = 1.45, C₅–C₆–C₇–C₈ = 25.9; (b) Ti–C₁ = 2.47, Ti–C₂ = 2.43, Ti–C₄ = 2.83, Ti–C₅ = 2.64, Ti–C₇ = 2.55, Ti–C₈ = 2.68, C₁–C₂ = 1.45, C₂–C₃ = 1.36, C₆–C₇ = 1.45, C₅–C₆–C₇–C₈ = 26.88.

geometrical parameters. Addition of polarization functions on carbon atoms does not affect significantly the predicted equilibrium geometries; see the captions of Figure 2 and Figure 3. The effects of electron correlation have been checked by performing a few test computations on the active species and on the preinsertion intermediate of butadiene homopolymerization using a method based on density functional theory (DFT). Again, they have confirmed the reliability of the ROHF/TZV/6-31G computations, at least as concerns the geometries of the stationary points involved in the reaction path. DFT computations have been performed with the Gaussian94 package,³⁷ using the hybrid B3LYP method for the exchange–correlation energy³⁸ and the LanL2DZ basis set.³⁹ If not

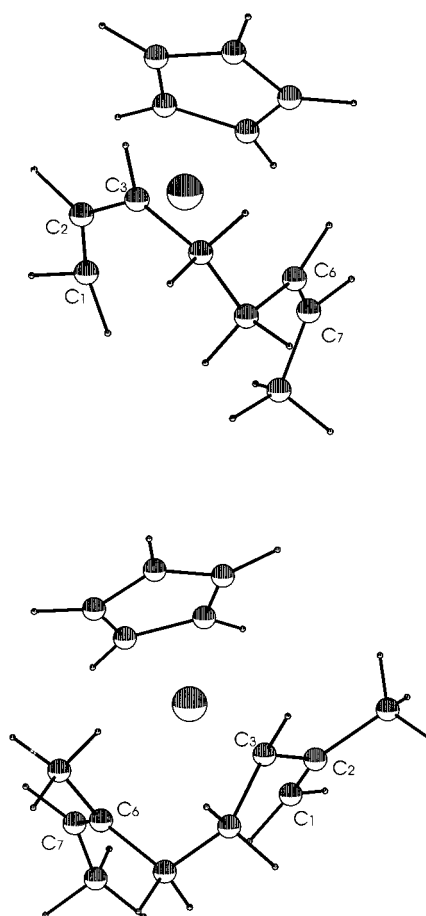


Figure 2. Optimized structures of the active species [CpTi–R₁]⁺ (a) and [CpTi–R₂]⁺ (b). Selected geometrical parameters (Å and deg) obtained at the ROHF/TZV/6-31G, (DFT-UHF/B3LYP/LanL2DZ), and [ROHF/TZV/6-31G*] level of computation: (a) Ti–C₁ = 2.16,(2.13),[2.17]; Ti–C₂ = 2.39,(2.32),[2.37]; Ti–C₃ = 2.75,(2.64),[2.70]; Ti–C₆ = 2.65,(2.55),[2.65]; Ti–C₇ = 2.83,(2.64),[2.78]; C₁–C₂ = 1.46,(1.46),[1.46]; C₂–C₃ = 1.36,(1.40),[1.36]; C₆–C₇ = 1.35,(1.37),[1.34]; (b) Ti–C₁ = 2.45; Ti–C₂ = 2.41; Ti–C₃ = 2.23; Ti–C₆ = 2.71; Ti–C₇ = 2.87; C₁–C₂ = 1.38; C₂–C₃ = 1.45; C₆–C₇ = 1.35.

explicitly specified, all energies reported in the text refer to single-point MP2 computations, corrected for BSSE, on nuclear configurations optimized at the SCF level.

Results

The Active Species. To find the optimum geometries of the active species, we start by locating the transition states for the endo–endo insertion of *cis*-butadiene into [CpTi(butenyl)]⁺ and that of *cis*-isoprene into [CpTi(isoprenyl)]⁺, with both allyls in the anti form. Since they will be used just as starting points for geometry optimizations, these computations have been carried out with the smaller 3-21G basis set.

The starting points for geometry optimizations are important because several minimum energy configurations are possible for the active species, and therefore it is important to locate those that are accessible from the saddle points of the insertion step. In fact, the

(37) Frisch, M. J.; Trucks, G. W.; Schlegel, H. B.; Gill, P. M. W.; Johnson, B. G.; Robb, M. A.; Cheeseman, J. R.; Keith, T.; Petersson, G. A.; Montgomery, J. A.; Raghavachari, K.; Al-Laham, M. A.; Zakrzewski, V. G.; Ortiz, J. V.; Foresman, J. B.; Cioslowski, J.; Stefanov, B. B.; Nanayakkara, A.; Challacombe, M.; Peng, C. Y.; Ayala, P. Y.; Chen, W.; Wong, M. W.; Andres, J. L.; Replogle, E. S.; Gomperts, R.; Martin, R. L.; Fox, D. J.; Binkley, J. S.; Defrees, D. J.; Baker, J.; Stewart, J. P.; Head-Gordon, M.; Gonzalez, C.; Pople, J. A. Gaussian, Inc.: Pittsburgh, PA, 1995.

(38) Becke, A. D. *J. Chem. Phys.* **1993**, *98*, 5648.

(39) (a) Hay, P. J.; Wadt, W. R. *J. Chem. Phys.* **1985**, *82*, 270. (b) Wadt, W. R.; Hay, P. J. *J. Chem. Phys.* **1985**, *82*, 284. (c) Hay, P. J.; Wadt, W. R. *J. Chem. Phys.* **1985**, *82*, 299.

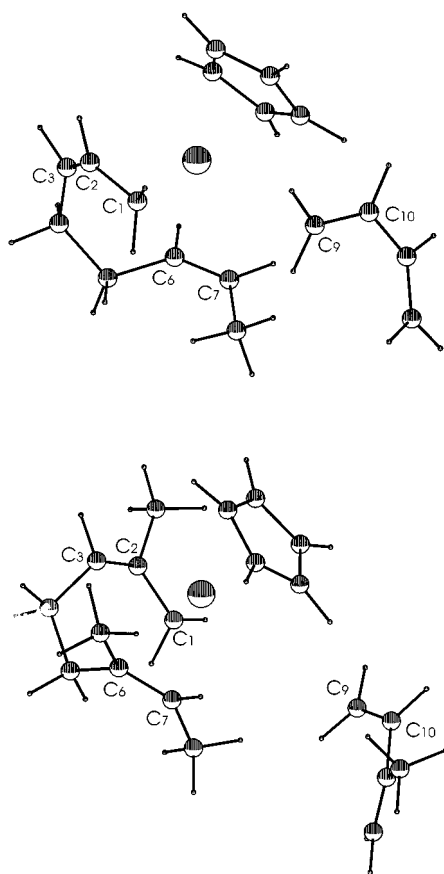


Figure 3. Minimum energy configuration for coordination of (a) butadiene to $[\text{CpTi-R}_1]^+$ and (b) isoprene to $[\text{CpTi-R}_2]^+$ (**C1**). Selected geometrical parameters (Å and deg), values in parentheses refer to DFT-UHF/B3Lyp/LanL2DZ computation: (a) $\text{Ti-C}_1 = 2.16, (2.18)$; $\text{Ti-C}_2 = 2.39, (2.36)$; $\text{Ti-C}_3 = 2.76, (2.76)$; $\text{Ti-C}_6 = 2.66, (2.63)$; $\text{Ti-C}_7 = 2.84, (2.76)$; $\text{Ti-C}_9 = 4.31, (2.79)$; $\text{Ti-C}_{10} = 4.60, (3.30)$; $\text{C}_1\text{-C}_2 = 1.47, (1.45)$; $\text{C}_2\text{-C}_3 = 1.36, (1.39)$; $\text{C}_6\text{-C}_7 = 1.35, (1.37)$; $\text{C}_9\text{-C}_{10} = 1.33, (1.37)$; $\text{C}_9\text{-C}_{10}\text{-C}_{11}\text{-C}_{12} = 32.4$; (b) $\text{Ti-C}_1 = 2.22$, $\text{Ti-C}_2 = 2.39$, $\text{Ti-C}_3 = 2.47$, $\text{Ti-C}_6 = 2.75$, $\text{Ti-C}_9 = 2.73$, $\text{Ti-C}_{10} = 4.74$, $\text{Ti-C}_{10} = 5.31$, $\text{C}_1\text{-C}_2 = 1.44$, $\text{C}_2\text{-C}_3 = 1.39$, $\text{C}_6\text{-C}_7 = 1.36$, $\text{C}_9\text{-C}_{10} = 1.33$, $\text{C}_9\text{-C}_{10}\text{-C}_{11}\text{-C}_{12} = 35.8$.

π -allylic coordination is quite a rigid one, especially in the presence of the back-biting interaction, so that the kinetic products are not expected to easily isomerize in other more stable minima, if any. That holds also for the preinsertion intermediate, as confirmed by the high-energy barrier (ca. 22 kcal/mol) found for the thermal isomerization of the endo–endo $\text{CpZr(allyl)(butadiene)}$ complex to the exo–exo one.^{25a} In addition, for isoprenyl, there are in principle two active species, which differ in the position of the methyl group. Thus, it is important to check which of the two adducts is preferentially formed starting from the transition state for insertion. Previous computations have shown that insertion of isoprene into the Ti-methyl bond yields the $\text{Ti-2-methylpentenyl}$ adduct,^{3a} and therefore, for the location of the transition state for insertion, the active species has been initially modeled by $[\text{CpTi-2-methylbuten-1-yl}]^+$.

The predicted nuclear configurations for the two saddle points are reported in Figure 1. For both nuclear configurations, all gradients are below the threshold of

1×10^{-4} hartree/bohr, and the Hessian matrixes have only one negative eigenvalue.

Postponing the discussion of the two transition states, we only remark that 2-methylbutadiene inserts into the Ti-allyl bond with the C_4 carbon, yielding the Ti-2-methylallyl adduct, in accordance with experimental results. Thus, the active species for butadiene and isoprene homopolymerization will be modeled by $[\text{CpTi-(R}_1)]^+$ ($\text{R}_1 = \text{octo-2,6-diene(1-yl)}$) and $[\text{CpTi(R}_2)]^+$ ($\text{R}_2 = \text{2,6-dimethylocto-2,6-diene(1-yl)}$), respectively, in the arrangement⁴⁰ resulting from the endo–endo insertion of *cis*-butadiene in $[\text{CpTi-(butadienyl)}]^+$ and *cis*-isoprene in $[\text{CpTi-(isoprenyl)}]^+$, cf. Figure 1.

Geometry optimizations of the species of Figure 1 lead to the minimum energy configurations of $[\text{CpTi(R}_1)]^+$ and $[\text{CpTi(R}_2)]^+$ shown in Figure 2. Both ending units are coordinated in the anti form, with the penultimate unit of R coordinated η^2 to the metal center, a back-biting interaction. The distances between Ti and the unsaturated carbons of the penultimate unit are in the range 2.65–2.87 Å for both R_1 and R_2 , and the π MOs are oriented in the ideal way to interact with the d orbitals of Ti , lying in the plane parallel to the cyclopentadienyl ring. In the caption of Figure 2 are also reported the results of test computations carried out with the addition of d type polarization functions on carbons and those obtained at DFT. As it can be seen, no relevant differences have been found.

The back-biting interaction causes a weakening of the Ti-butenyl bond. The ending unit of R_1 is not coordinated to Ti as an ideal $\eta^3\text{-}\pi$ allyl ligand, but its coordination mode is somewhat distorted toward a $\eta^1\text{-}\sigma$ one. The Ti-C_1 and the Ti-C_3 , cf. Figure 2, bond distances are 2.16 and 2.75 Å, respectively, and become 2.17 and 2.70 Å after adding a d type polarization function on carbons and 2.13 and 2.64 Å at the DFT level. On the contrary, for $[\text{CpTi(R}_2)]^+$ the same Ti-C distances are 2.45 and 2.23 Å, respectively, as expected for a slightly distorted $\eta^3\text{-}\pi$ coordination. Thus, R_2 is more strongly bound to $[\text{CpTi}]^{2+}$ than R_1 ; ab initio computations predict that the two binding energies differ by ca. 10 kcal/mol.

The unpaired electron occupies a nonbonding level, whose major contribution comes from the 4s orbital of Ti . No relevant variations will be observed along the reaction path.

Coordination of Monomer to the Active Species.

The minimum energy configurations for the coordination of butadiene and isoprene to the active species $[\text{CpTi(R}_1)]^+$ and $[\text{CpTi(R}_2)]^+$ (**C1**) are shown in Figure 3.

For both complexes, M is significantly more distant from Ti than R , especially for $[\text{CpTi(R}_2)(\text{isoprene})]^+$. The back-biting interaction prevents a closer approach of M to the active species, because of the electronic repulsions between the π orbitals of M and R . To minimize them, M takes a nonplanar geometry, with a dihedral angle of ca. 32°, so that only two carbons are close to Ti . Nonetheless, the approach of isoprene to $[\text{CpTi(R}_2)]^+$

(40) We prefer to use the term arrangement in this context because the term conformation could be misleading when used for the ending units of P . In fact, both the ultimate and the penultimate unit of P are rigidly fixed to the metal ion, so that interconversion between two conformations cannot occur by simply rotating about a single bond.

Table 1. Relative Energies (kcal/mol) of the Stationary Points for Homopolymerization of Butadiene and Isoprene^a

		C1	T1	C2	T2	C1 ^b
butadiene	SCF	-2.88	+13.22	+3.31	+16.79	-2.90
	MP2	-5.72	+9.60	-4.04	-2.92	-4.97
isoprene	SCF	-1.88	+23.02	+4.46		
	MP2	-0.76	+23.34			

^a Notes: Relative energies refer to the sum of the SCF (MP2) energies (hartree) of the active species and of the monomer, both corrected for BSSE: butadiene -154.86161 (-154.97498); isoprene -193.88394 (-194.09105); [CpTi(R₁)]⁺ -1350.78326 (-1351.28324); [CpTi(R₂)]⁺ -1428.82485 (-1429.51465). ^b Isoprene coordinated to [CpTi(R₁)]⁺.

causes a significant rearrangement of the η^3 coordination mode of R₂, which is still of η^3 - π allylic type, but with the C₁ carbon now nearest to Ti, in the right position to give the products of 1,4 insertion.

The shortest distance between the monomer carbons and Ti is 4.7 Å for isoprene and 4.3 Å for butadiene, cf. Figure 3, suggesting that the latter monomer is more strongly bound to the metal center than the former, as confirmed by the coordination energies of butadiene to [CpTi(R₁)]⁺ and isoprene to [CpTi(R₂)]⁺, which are -5.7 and -3.7 kcal/mol, respectively, cf. Table 1. Addition of d type polarization functions to carbons does not change the situation; the shortest Ti-C_m distance is 4.35 for [CpTi(R₁)(butenyl)]⁺, cf. Figure 3, and the orientation of the two moieties is very similar to that of Figure 3. On the other hand, the Ti-M distances are predicted to be much shorter at the DFT level, surprisingly comparable with those obtained at the ROHF/3-21G level of approximation. This is probably due to the flatness of the PES in the region of relatively long Ti-M distances, as confirmed by a few single-point computations for the rigid approach of M to Ti, which have shown that decreasing the Ti-C₉ interatomic distance up to 2.9 Å requires only 2.3 kcal/mol at the ROHF level.

A wide scan of the PES, performed with the smaller 3-21G basis set, has shown that the approach of M to Ti affects initially the η^3 coordination mode of the allyl group. For the [CpTi(butenyl)(butadiene)]⁺, upon decreasing the Ti-C₉ distance up to 2.6 Å, the back-biting interaction is still retained and the energy increases by ca. 6 kcal/mol, whereas at 2.4 Å, the back-biting interaction is broken and the potential energy quickly increases.

The potential energy hypersurface (PES) in this region of the nuclear coordinates is very flat for both [CpTi(butenyl)(butadiene)]⁺ and [CpTi(isoprenyl)(isoprene)]⁺, because the change of the allyl coordination mode and the loss of the back-biting interaction give rise to a linear chain of eight carbons, which is σ bound to Ti and has therefore a high conformational flexibility. That makes it difficult to locate the true transition state connecting the regions of PES corresponding to longer and shorter Ti-M distances. We have been able to find a flat region of the PES in which all gradients are below the threshold of 1×10^{-3} hartree/bohr, which has been often adopted in the literature for systems like the present one, but we were unable to locate a true transition state, for both [CpTi(R₁)(butadiene)]⁺ and [CpTi(R₂)(isoprene)]⁺.

The energy barriers estimated by those scans of the PES are ca. 15 kcal/mol for [CpTi(R₁)(butadiene)]⁺ and

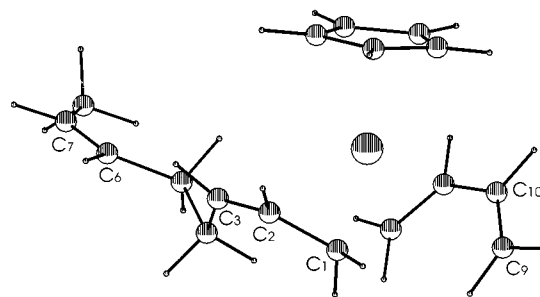


Figure 4. Minimum energy configuration for the π dienilic (η^4) coordination of butadiene to [CpTi-R₁]⁺. Selected geometrical parameters (Å and deg): (a) Ti-C₁ = 2.15, Ti-C₂ = 2.43, Ti-C₃ = 2.54, Ti-C₆ = 5.31, Ti-C₇ = 6.42, Ti-C₉ = 3.19, Ti-C₁₀ = 2.84, C₁-C₂ = 1.48, C₂-C₃ = 1.35, C₆-C₇ = 1.33, C₉-C₁₀ = 1.34.

ca. 24 kcal/mol for [CpTi(R₂)(isoprene)]⁺. To our knowledge, there are no experimental estimates of the activation energies for butadiene and isoprene homopolymerizations in the presence of CpTiCl₃-MAO. For styrene homopolymerization, which is faster than that for butadiene, the activation energy is 7.6 kcal/mol,^{19a} thus suggesting that the above values are probably overestimated. However, as it will be seen, an accurate estimate of the heights of these barriers is not essential for outlining a reasonable mechanistic scheme and is therefore beyond the aims of the present work.

The Preinsertion Intermediates. After crossing the early transition state for coordination of M to the metal ion, two different reaction paths are possible: the direct insertion of M into the Ti-R bond (one-step mechanism) and the relaxation in another stationary point, where M is now more tightly bound to Ti at the expense of the Ti-R bond (two-step mechanism). To check for either possibility, we have carried out geometry optimizations starting from shorter Ti-M distances. The stationary points **C2**, whose relative energies are reported in Table 1, have been obtained. For [CpTi(R₁)(butadiene)]⁺, as well as for [CpTi(R₂)(isoprene)]⁺, M is now coordinated η^4 to Ti, the back-biting interaction has been lost, and the η^3 π allylic coordination is partially restored, although it is always significantly distorted toward the η^1 coordination mode, cf. Figure 4.

For [CpTi(R₁)(butadiene)]⁺, that stationary point falls ca. 1 kcal/mol above **C1**, cf. Table 1; for [CpTi(R₂)(isoprene)]⁺ the computation has been done only at the SCF level, and the energy difference from **C1** is 6.5 kcal/mol, very similar to that of butadiene at the same level of computation.

The Insertion Step. The transition state for the insertion of butadiene into the Ti-R₁ bond (**T2**), starting from the **C2** minimum, with M coordinated η^4 to Ti, is shown in Figure 5. There are no significant differences from the transition state of Figure 1a, where R₁ was replaced by a single butenyl unit, both in the geometrical parameters and in the activation energies. Thus, we will refer to the two transition states shown in Figure 1, with R modeled by only one repeating unit.

The geometries of the activated states for butadiene and isoprene insertion are very similar to each other. Both monomers are coordinated to Ti with one of the two inner carbons, that are bound to the carbon which

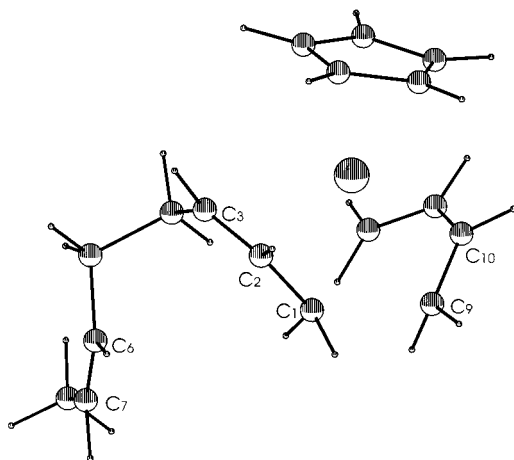


Figure 5. Transition state (**T2**) for insertion of butadiene into the Ti-R₁ bond. Selected geometrical parameters (Å and deg): Ti-C₁ = 2.46, Ti-C₂ = 2.42, Ti-C₃ = 2.67, Ti-C₆ = 5.21, Ti-C₇ = 6.06, Ti-C₉ = 2.60, Ti-C₁₀ = 2.25, Ti-C₁₁ = 2.54, Ti-C₁₂ = 2.81, C₁-C₂ = 1.46, C₂-C₃ = 1.35, C₆-C₇ = 1.33, C₉-C₁₀ = 1.41.

will insert in the Ti-R bond, much closer to the metal center than all the others. The distance between the two carbons that form the new C-C bond is 2.2 Å, as in previous accurate ab initio computations for polymerization of monoalkenes with biscyclopentadienyl titanocenes and zirconocenes.^{2,41}

The geometry of M is slightly distorted as a result of the mixing of the HOMO and LUMO of M, prior to M insertion. As pointed out by Hoffmann et al.,³⁶ the HOMO-LUMO mixing is important, because it lowers the contribution of the M carbon which forms the new C-C bond from the HOMO of M, decreasing the repulsive interactions between filled molecular orbitals of R and M.

Inspection of Figures 1 and 5 shows that the transition state for M insertion is stabilized by the interaction of Ti with the C₂-C₃ π bond of the ending unit of R: the distance Ti-C₃ is shorter than in **C2**, and the double bond is slightly elongated. This dative bond will give rise to the back-biting interaction after insertion has occurred. Starting from **C2**, the computed barrier for the insertion of butadiene into the σ Ti-R₁ bond is 1.1 kcal/mol. For insertion of isoprene into the Ti-isoprenyl bond we refer to 3-21G computations, which predict no barrier for isoprene insertion, as well as for butadiene.

Butadiene-Isoprene Copolymerization. For a better understanding of the factors responsible for the observed differences in the rates of butadiene and isoprene homopolymerizations, we have studied the coordination of isoprene to [CpTi(R₁)]⁺. The minimum energy structure for coordination of isoprene to [CpTi(R₁)]⁺ is shown in Figure 6; the coordination energy is reported in Table 1. There are no remarkable differences between the minimum energy structures of [CpTi(R₁)-(isoprene)]⁺ and [CpTi(R₁)(butadiene)]⁺. In fact, the degree of η^1 distortion of R₁ is essentially the same for either complex, and the two monomers take essentially the same nuclear configurations in the two coordination minima. Remarkably, the energy gain for coordinating

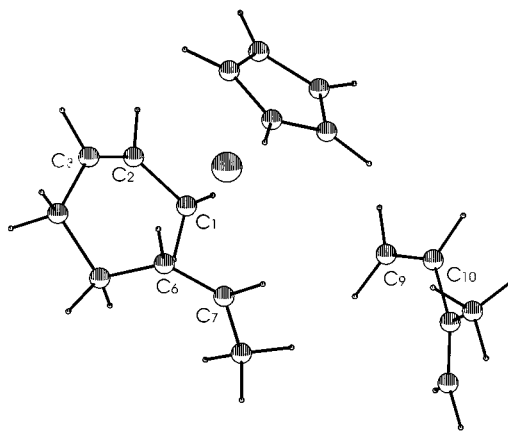


Figure 6. Minimum energy configuration for coordination of isoprene to [CpTi-R₁]⁺ (C1 for copolymerization). Selected geometrical parameters (Å and deg): Ti-C₁ = 2.16, Ti-C₂ = 2.39, Ti-C₃ = 2.76, Ti-C₆ = 3.47, Ti-C₇ = 3.68, Ti-C₉ = 4.18, Ti-C₁₀ = 4.62, C₁-C₂ = 1.47, C₂-C₃ = 1.36, C₆-C₇ = 1.35, C₉-C₁₀ = 1.33, C₉-C₁₀-C₁₁-C₁₂ = 35.25.

isoprene to [CpTi(R₁)]⁺ is ca. 4.97 kcal/mol, very similar to that for coordination of butadiene and ca. 4.2 kcal/mol more exoergonic than that predicted for coordination of isoprene to [CpTi(R₂)]⁺.

This result, together with the finding that the insertion step is practically activationless, confirms that the rate of homopolymerization of conjugated diolefins in the presence of the CpTiCl₃-MAO catalytic system is controlled by the ending unit of the growing polymer chain and explains why, despite of the large difference in the homopolymerization rates, butadiene and isoprene copolymerize randomly, see below.

Discussion

The results obtained so far can be summarized as follows: (i) the growing polymer chain is coordinated to the Ti ion both with its allylic ending unit and with the π bond of the penultimate unit, a back-biting interaction; (ii) the approach of M to Ti, at distances short enough for insertion occur, requires the breakage of the back-biting interaction and the switch of the η^3 - π allylic coordination mode toward the η^1 - σ one; (iii) the insertion of M into the σ Ti-R bond is predicted to be an easy process, requiring a very low activation energy, if any, so that the polymerization rates appear to be mainly determined by the rearrangement of the ending units of P coordinated to the metal ion, prior to M insertion; (iv) the great difference in the rates of isoprene and butadiene polymerization appears to be due to the very different strengths of the η^3 Ti-butenyl and Ti-isoprenyl coordination bonds.

As concerns point (i), the back-biting interaction is formed during the insertion of a new monomer in the growing polymer chain, cf. Figures 1 and 5, and there is no need for this quite strong interaction (roughly 10 kcal/mol) to be lost after the new C-C bond is formed, as confirmed by geometry optimizations performed on the structures of Figure 1, which lead to the minimum energy configurations for the active species shown in Figure 2. The back-biting interaction certainly has a part in determining the configuration of the polymerization products, since it stabilizes the anti form over

(41) (a) Sakay, S. J. *J. Phys. Chem.* **1994**, *98*, 12053. (b) Jensen, V. R.; Børve, K. J.; Ystenes, M. *J. Am. Chem. Soc.* **1995**, *117*, 4109.

the syn one by ca. 10 kcal/mol. Therefore, it is not necessary to invoke that the incoming monomer is coordinated in the cis form and that there is a high barrier for the syn–anti isomerization to explain why both butadiene and isoprene give cis polymers; the back-biting interaction is formed during the insertion step, independently of M conformation, and forces the new ending unit of R to take the anti form.

The back-biting interaction also affects the coordination step, forcing M to be weakly coordinated (η^2) to the active species. That step is exoergonic for both butadiene and isoprene homopolymerization, but the energy gain is significantly larger for the former than for the latter. Our computations suggest that this difference is to be ascribed to the active species rather than to M and, in particular, to the ending unit of R, as suggested by the predicted energy change for coordination of isoprene to $[\text{CpTi}(\text{R}_1)]^+$ and to $[\text{CpTi}(\text{R}_2)]^+$. Accordingly, the Ti–butenyl bond is significantly different from the Ti–isoprenyl one, whereas no significant differences have been found for the back-biting interaction in R_1 and R_2 , cf. Figures 2 and 3. In the case of R ending with an isoprenyl unit, the three allyl carbons are roughly equidistant from Ti, as one should expect for an ideal π allylic coordination bond, whereas in the case of a butenylic ending unit, the η^3 – π allylic coordination is strongly distorted toward a σ bond. That difference can be explained by resorting to interaction diagrams and second-order perturbation theory.⁴³ The methyl group of isoprenyl slightly raises the energy of the HOMO-1 of allyl (ca. 9 kcal/mol), which can better interact with the LUMO of $[\text{CpTi}]^{2+}$, increasing the strength of the Ti–allyl bond.^{3a} As a consequence, the isoprenyl unit is coordinated η^3 to Ti, as an ideal π allylic ligand, whereas the coordination mode of the butenyl unit, being weaker, can be more easily distorted toward the η^1 one. That difference has important consequences on the electrophilicity of the active species. In fact, the $\eta^3 \rightarrow \eta^1$ switch of the coordination mode of R decreases the energy of the LUMO of the active species, which mostly contributes to bind M.^{3a}

It is surprising that the weak coordination of M to the active species mostly affects the coordination mode of the ending unit of R, leaving unaltered the back-biting interaction. The former interaction is in fact stronger than the latter, as expected from the standard rule of valency, since the π allyl group formally carries a negative charge, but it is somewhat more flexible. The η^3 – π allylic coordination mode can be thought of as the limiting form of two resonance structures, involving a strong σ Ti–C bond and a relatively weaker dative bond between the filled π MO of the allyl and an empty d orbital of Ti. The breakage of the latter will reinforce the former, and therefore the $\eta^3 \rightarrow \eta^1$ rearrangement is predicted to be energetically less expensive than the breakage of the back-biting interaction. Indeed, there are several examples in the literature of transition metal complexes with one or two allyl ligands coordinated η^1 to the metal ion.⁴⁴

In the coordination complex, the incoming monomer and the ending unit of the growing polymer chain are still far from each other. Ab initio computations predict that the minimum energy path for M insertion goes through a maximum energy structure in which R is coordinated η^1 to the metal center. That step is predicted to be the rate-determining step of the whole propagation reaction. The activation energy is higher for homopolymerization of isoprene than for butadiene, because of the already mentioned difference in the coordination mode of the two allyls. The chemoselectivity of the propagation reaction is also determined at this stage and depends on which of the two resonant forms of the π allyl ligand becomes the most stable one. Both steric and electronic effects can control the $\eta^3 \rightarrow \eta^1$ rearrangement: steric hindrances of the two methyl groups probably play a role in preventing the formation of the σ bond at C_1 in the homopolymerization of 4-methyl-1,3-pentadiene,^{3b} but electronic effects are also important, as testified by the fact that, in all the monomers studied, the $\eta_3 \rightarrow \eta_1$ rearrangement always yields the most substituted double bond, going through the less substituted carbanion.

The hypothesis that the $\eta^3 \rightarrow \eta^1$ transition is the rate-determining step for polymerization of butadiene has indeed been suggested also for other catalysts, for instance η^3 -allylnickel trifluoroacetate⁴⁵ and $[(\text{C}_4\text{H}_7)\text{-PdCl}_2]$.^{12,13} In the latter case the reaction is slow enough to be followed by NMR; the results suggested that, upon butadiene coordination, the η^3 C_4H_7 –Pd bond rearranges toward a σ – η^1 coordination. Subsequently, butadiene inserts into the σ Pd–allyl bond and the π allylic coordination is restored. In the presence of the latter catalyst, the ΔG for the $\eta^3 \rightarrow \eta^1$ rearrangement of an isoprenylic unit is ca. 2 kcal/mol larger than for butenyl. The same trend is also observed in the presence of Pt(II)-⁴⁶ and Ir(III)-⁴⁷-based catalysts. Thus, our results agree with the general finding that homopolymerization of isoprene by transition metal catalysts is, in similar conditions, slower than that of butadiene. That is indeed the behavior observed in the presence of other catalytic systems, such as $\text{TiI}_4\text{Al}(\text{alkyl})_3$,¹⁴ VCl_3 – $\text{Al}(\text{alkyl})_3$,¹⁵ $((\text{C}_4\text{H}_7)\text{Ni})_2$,¹⁶ and $\text{Co}(\text{acac})_2$ – $\text{Al}(\text{alkyl})_3$.⁴⁸ To our knowledge, there is only one catalyst, $(\text{CoI}-\text{Al}_2\text{OC}_2\text{H}_5)$,⁴⁹ in the presence of which isoprene homopolymerization is faster than that for butadiene.

The mechanistic scheme proposed here can also explain why the reactivity ratios observed for butadiene and isoprene copolymerization in the presence of Cp-TiCl_3 – MAO ^{17b} are close to unity. The reactivity ratio $r_{ij} = k_i/k_{ij}$ is the ratio of the rate constants for the insertion of two different monomers M_i and M_j into the Ti– R_i bond, where R_i is the growing chain whose ending

(42) (a) Lauher, J. W.; Hoffmann, R. *J. Am. Chem. Soc.* **1976**, *98*, 1729–1742. (b) Thorn, D. L.; Hoffmann, R. *J. Am. Chem. Soc.* **1978**, *100*, 2079.

(43) (a) Hoffmann, R. *Acc. Chem. Res.* **1971**, *4*, 1. (b) Libit, L.; Hoffmann, R. *J. Am. Chem. Soc.* **1974**, *96*, 1370.

(44) (a) Erker, G.; Berg, K.; Angermund, K.; Krueger, K. *Organometallics* **1987**, *6*, 2620–1, and references therein. (b) Hoffmann, E. G.; Kallweit, R.; Schroth, G.; Seevogel, K.; Stempf, W.; Wilke, G. *J. Organomet. Chem.* **1975**, *97*, 183–202. (c) Chodosh, D. F.; Katahira, D. J. *J. Organomet. Chem.* **1980**, *187*, 227–231. (d) Mason, R.; Russel, D. R. *Chem. Commun.* **1965**, 26.

(45) Warin, R.; Julemont, M.; Teyssié, Ph. *J. Organomet. Chem.* **1980**, *185*, 413.

(46) McDouals, W. S.; Mann, B. E.; Raper, G.; Shaw, B. L.; Shaw, G. *Chem. Commun.* **1969**, 1254.

(47) Powell, J.; Shaw, B. L. *J. Chem. Soc. A* **1968**, 780.

(48) Pasquon, I.; Porri, L.; Zambelli, A.; Ciampelli, F. *Chim. Ind.* **1963**, *43*, 509.

(49) Dawans, F.; Theyssié, Ph. *Eur. Polym. J.* **1941**, *5*, 1969.

unit derives from the insertion of M_i , and k_{ij} is the rate constant of the reaction



According to our results, the value of r_{ij} depends critically on R_i , thus explaining why, despite the large difference in the homopolymerization rates, the reactivity ratios for butadiene and isoprene copolymerization are almost unity. Reactivity ratios on the order of unity are observed for isoprene and butadiene also in the presence of $\text{Co}(\text{acac})_2\text{-Al}(\text{alkyl})_3$.⁴⁸

Conclusion

The results hereby presented provide evidence that, in the presence of $\text{CpTiCl}_3\text{-MAO}$ catalysts, polymerization of conjugated dienes could occur with a mechanism that is similar to the σ mechanism first proposed by Arlman for polymerization of diolefins in the presence of heterogeneous catalysts.⁵⁰ The rate-determining step is the coordination of an incoming monomer to the active catalytic species with the simultaneous switching of the

R coordination mode from $\eta^3\text{-}\pi$ to $\eta^1\text{-}\sigma$. The subsequent insertion of M into the σ Ti-R bond is predicted to be a comparatively much easier process.

Of course, further computational refinements are needed for a definitive assessment of the reaction mechanism. Preliminary computations at the DFT level have not shown relevant discrepancies with the proposed mechanistic scheme, cf. Figures 2 and 3 and ref 5b. We only remark that, although the computational level adopted is probably not able to give very accurate energy differences between the hypothesized stationary states, the proposed mechanistic scheme appears to be able to rationalize a certain number of experimental facts, e.g. the very different reactivity of the isoprene and butadiene, the different behavior of 4-methylbutadiene, which at variance with butadiene and isoprene yields the products of 1,2 insertion, and the fact that reactivity ratios for butadiene and isoprene copolymerizations are near unity. Finally, the mechanistic picture emerging from our computations is in line with that suggested by NMR experiments for butadiene homopolymerization in the presence of $[(\text{C}_4\text{H}_7)\text{PdCl}_2]$.

Acknowledgment. The financial support of MURST and Italian CNR is gratefully acknowledged.

(50) Arlman, E. J. *J. Catal.* **1966**, 5, 178–189.

OM980940G